Absence of magic-angle effects in the intralayer resistance R_{xx} of the quasi-one-dimensional organic conductor $(TMTSF)_2ClO_4$

W. Kang*
Department of Physics, Ewha W. University, Seoul 120-750, Korea
(Received 18 July 2007; published 13 November 2007)

We measured both intralayer (R_{xx}) and interlayer (R_{zz}) magnetoresistances on the same sample of the quasi-one-dimensional organic superconductor $(TMTSF)_2ClO_4$. When the possible buildup of the electrostatic potential difference along the interlayer direction was properly prohibited, the intralayer resistance R_{xx} did not show any magic-angle effect. However, when R_{xx} was measured again on the same sample but with a conventional electrical contact configuration, it showed the magic-angle effect much like in R_{zz}. We conclude that the magic-angle effects are essentially the interlayer charge transfer phenomena.

DOI: 10.1103/PhysRevB.76.193103 PACS number(s): 71.18.+y, 72.15.Gd, 74.70.Kn

When the magnetic field is applied to the quasi-one-dimensional (Q1D) organic conductors $(TMTSF)_2X$ [TMTSF=tetramethyltetrathiafulvalene], various types of magic-angle effects (MAEs) occur when the orientation of the magnetic field is changed with respect to the crystal. Lebed magic-angle resonances have been observed under rotation of the field in the plane perpendicular to the one-dimensional (1D) axis (a axis),[1–4] and Danner-Kang-Chaikin (DKC) oscillations under rotation of the field in the plane defined by the 1D axis and the normal of the layers.[5,6] The third angular effect (TAE) was observed in the case of field rotation in the layer plane.[7,8] For a generic direction of the magnetic field, a mixture of aforementioned phenomena could be observed.[9–11] Experimentally, one of the most recent advance for the MAEs is the three-dimensional reconstruction of the magnetoresistance, which showed that the Lebed resonance is the only fundamental angular effect and that the other effects result from the modulation of its amplitude.[11]

There has been numerous theoretical works to explain the magic-angle effects in the interlayer conduction.[12–27] Some of them are based on the semiclassical Boltzmann transport equation,[7–9,14,18,28] some on the quantum mechanical Kubo-type formula,[23,26,29] and the others on the phase coherence in interlayer electron tunneling.[15,19–22,24,27] Although based on different mechanisms, all of the above models produced similar results, and hence, it is not straightforward to identify the underlying physics of the MAEs.

It is well believed that the observed MAEs are more pronounced in R_{zz} than in R_{xx}. Moreover, there is even a controversy for the existence of the MAEs in R_{xx}.[4] $(TMTSF)_2X$ is a strongly anisotropic conductor with a typical conductivity anisotropy of $\sigma_a:\sigma_b:\sigma_c=25:1:10^{-3}$.[30] When one takes a rectangular sample of anisotropic material with dimensions ℓ_1, ℓ_2, ℓ_3 and with resistivities ρ_1, ρ_2, ρ_2, respectively, along each direction, the sample can be mapped to an equivalent isotropic sample of dimensions ℓ_1', ℓ_2', ℓ_3' and of isotropic resistivity ρ, where $\ell_i'=\ell_i(\rho_i/\rho)^{1/2}$ and $\rho^3=\rho_1\rho_2\rho_3$.[31–33] Then, the equivalent sample dimension along the least conducting interlayer direction is the largest in most of the cases, and the possibility that R_{xx} contains some portion of R_{zz} cannot be fully excluded unless a careful consideration is given to make electrical contacts.

In order to remove the ambiguity residing on the MAEs in R_{xx}, we measured both R_{xx} and R_{zz} on the same sample in a special way to separate the two components as well as we can. The following strategy had been employed to avoid any mistakenly drawn conclusion. First, taking a pristine sample, electrical contacts were applied to measure R_{xx} with the carbon paste as shown in Fig. 1(a). Potential contamination of the R_{zz} component into R_{xx} was minimized by carefully covering the side with paste and, therefore, by short-circuiting any possible potential difference built along the interlayer direction. (Hereafter, we call it $R_{xx}^{(I)}$.) After a complete set of measurements at low temperature and in the magnetic field, the sample was recovered and thoroughly washed out of the paste. The sample was then cut into two pieces, of which the longer piece was used to measure R_{xx} again, but in the conventional way of making contacts [Fig. 1(b)] (hereafter, we call it $R_{xx}^{(II)}$), and the shorter piece was used to measure $R_{zz}^{(II)}$ in order to probe the sample quality [Fig. 1(c)]. Another piece of the sample from the same batch was mounted in the R_{zz} measurement configuration through the experiments and used as a reference.

Although the sample is in its most pristine condition when $R_{xx}^{(I)}$ is measured, it did not show any MAEs. On the other

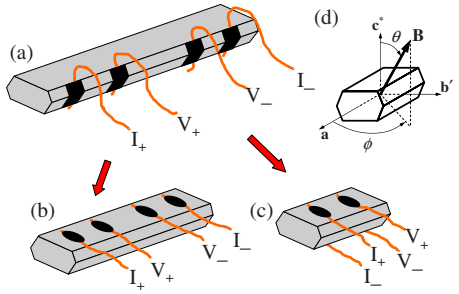

FIG. 1. (Color online) Configurations of electrical contacts for R_{xx} and R_{zz} measurements used in this study. Initially, four contacts were made on a side of the sample to measure $R_{xx}^{(I)}$, with any spurious voltage drop along the z axis shorted (a). After having completed the $R_{xx}^{(I)}$ measurements, the contacts were removed and the sample was thoroughly cleaned of the paste. The sample was then cut into two pieces, of which (b) the longer one was used to measure $R_{xx}^{(II)}$ with the conventional contact configuration and (c) the shorter one to measure R_{zz}. The directions and angles are defined in (d).

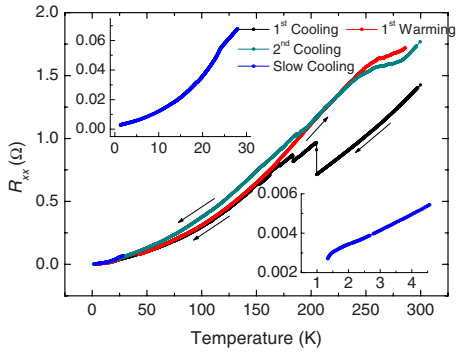

FIG. 2. (Color online) Cooling curves of the pristine $R_{xx}^{(\mathrm{I})}$ sample. The upper left inset shows the resistance behavior across the anion ordering transition around 24 K, and the lower right inset the onset of the superconducting transition.

hand, $R_{xx}^{(\mathrm{II})}$ of the recycled sample with conventional contact arrangement showed all the MAEs (in spite of numerous resistance jumps on cooling). R_{zz} always showed MAEs. This observation allowed us to conclude that the MAEs are absent in the R_{xx} and that they are purely the interlayer charge transfer phenomena.

Electrical contacts were applied to the samples using 20 μm annealed gold wires attached with carbon paste. A conventional four-wire ac lock-in method was used to measure the sample resistance. Cooling rate from 26 to 14 K was controlled to be 10 mK/min for all measurements in order to obtain a well anion-ordered state. All the angle dependent data presented in this Brief Report were obtained with a two-axis goniometer probe placed in a pumped helium bath (T = 1.5 K) and in a fixed magnetic field (H=10 T). The data at 6 T are essentially the same except for the smaller amplitude of anomalies and except for the absence of the field-induced spin-density wave (FISDW) over the whole angular range.

Figure 2 shows temperature dependence of R_{xx} of the pristine sample during two successive coolings. The sample suffered from a few minor resistance jumps between 150 and 200 K during the first cooling, and the resulting resistance increase became permanent. The increase of resistance at room temperature after two temperature cycles down to 1.5 K was less than 20% of its initial value. At a zero magnetic field, the beginning of the superconducting transition could be observed at 1.5 K after the slow cooling (lower right inset of Fig. 2). Residual resistance ratio (RRR) from the beginning of the measurement and right before the superconducting transition was as high as 470 in spite of the presence of a few jumps. Judging from the large value of RRR, the sharp decrease of resistance across the anion ordering transition (upper left inset of Fig. 2), and the high superconducting transition temperature, we could say that the sample quality was not degraded in spite of a few resistance jumps it suffered during cooling.

Figure 3 shows an equirectangular projection of the density plot of $R_{xx}^{(\mathrm{I})}(\theta,\phi)$ at 10 T. $R_{xx}^{(\mathrm{I})}(\theta,\phi)$ has only very weak and smooth ϕ dependence. None of the three major MAEs are present in these data. Variation of $R_{xx}^{(\mathrm{I})}(\theta{=}90°,\phi)$ with respect to the azimuthal angle ϕ is almost sinusoidal, with an

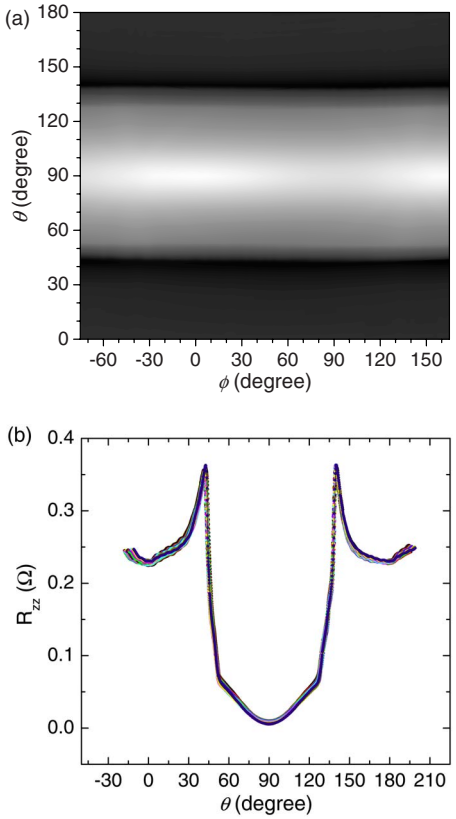

FIG. 3. (Color online) (a) Equirectangular projection of $R_{xx}^{(\mathrm{I})}(\theta,\phi)$ of the pristine sample under a magnetic field of 10 T. The sample resistance is represented on a logarithmic gray scale, with black for the largest resistance (0.4 Ω) and white for the lowest (0.005 Ω). The region where $\theta \lesssim 45°$ and $\theta \gtrsim 135°$ is dark because the sample is in the resistive FISDW state. (b) Raw data curves of $R_{xx}^{(\mathrm{I})}(\theta,\phi)$ versus theta show that the curves for 81 different ϕ values lie almost one above the other.

amplitude of about 1/3 of its average on ϕ. We can compare this result with $R_{zz}(\theta,\phi)$ of a pristine sample measured side by side during the same run and presented in Fig. 4. All three resonance phenomena are clearly present in R_{zz}. The bright lines emerging from the a axis (θ=90°, ϕ=0° and 180°) are the Lebed resonances. The pattern around the a axis represents the DKC oscillations and the TAE arising from the modulation of the Lebed resonances.[11] Although the useful data are limited within ±45° from the conducting plane (θ = 90°), all the Lebed resonances can be clearly distinguished and their modulation upon approaching the Q1D axis is also manifest.[11]

Absence of MAEs in $R_{xx}^{(\mathrm{I})}(\theta,\phi)$ is striking in view of the previous results in $(\mathrm{TMTSF})_2\mathrm{ClO}_4$ and $(\mathrm{TMTSF})_2\mathrm{PF}_6$, where clear Lebed resonances could be observed even in a weaker magnetic field than the field we used. In view of the current experimental condition, the experimental environments, both the temperature and the magnetic field, were optimal to observe the resonances if there are any, and the sample for $R_{xx}^{(\mathrm{I})}$ was in its most pristine state, in which we could study the Fermi surface effects in detail. However, it is still too premature to generalize the idea that there are no

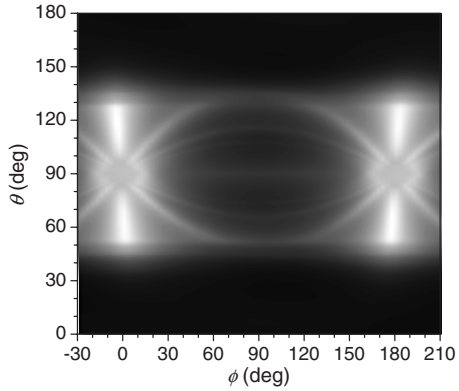

FIG. 4. Equirectangular projection of $R_{zz}(\theta,\phi)$ of the pristine sample under a magnetic field of 10 T. The sample resistance is represented on a logarithmic gray scale, with black for the largest resistance (220 Ω) and white for the lowest (0.33 Ω). The region where $\theta \lesssim 45°$ and $\theta \gtrsim 135°$ is dark because the sample is in the resistive FISDW state.

Lebed resonances and related resonant phenomena in R_{xx}.

In order to remove the ambiguity on the absence of MAEs in the $R_{xx}^{(\mathrm{I})}(\theta,\phi)$, the sample was warmed to ambient temperature, thoroughly cleaned of paste, cut into two pieces, and reconfigured to measure R_{xx} and R_{zz}, as explained in the experiment. The cooling rate was controlled to be identical to that in the first experiment. This time, the R_{xx} sample suffered from numerous resistance jumps due to the so-called microcracks. The RRR was reduced to 23, and the superconducting transition temperature was slightly lowered to 1.4 K. On the other hand, the sample piece in the R_{zz} configuration did not show any resistance jump as in the first experiment.

Figure 5(a) shows the $R_{xx}^{(\mathrm{II})}(\theta,\phi)$ measured from the longer piece of the sample with the conventional contact configuration, i.e., without short-circuiting the two *ab* planes. This time, R_{xx} contains clearly all the ingredients of MAEs in the same way as $R_{zz}^{(\mathrm{II})}$ [Fig. 5(b)], which was measured from the shorter piece left and which exhibited the MAEs as good as those in the pristine sample although it is temperature cycled three times before being measured.

The presence of good quality MAEs both in $R_{xx}^{(\mathrm{II})}$ and in $R_{zz}^{(\mathrm{II})}$ assures that the sample was in good quality when $R_{xx}^{(\mathrm{I})}$ was measured. Then, the absence of MAEs in $R_{xx}^{(\mathrm{I})}$ cannot be attributed to poor sample quality. Instead, the only plausible explanation is the absence of MAEs in R_{xx}, in general. Considering the large conductivity anisotropy in these materials, it is not unlikely that the experimentally measured R_{xx} contains some R_{zz} component unless the electrode configuration is optimized or if the current path is no longer ideal due to microcracks.

Finally, the data in Fig. 4 can be redrawn in a three-dimensional stereoscopic way as in Fig. 1 of Ref. 11 or in alternative coordinates as in Fig. 2 of Ref. 27. A similar figure could be generated from an analytic representation of the interlayer magnetoresistance, for example, Eq. (2) of Ref. 11. However, a detailed pattern is less resolved in the $(\mathrm{TMTSF})_2\mathrm{ClO}_4$ than in its sister compound $(\mathrm{TMTSF})_2\mathrm{PF}_6$. We would like to mention that exactly the same pattern,

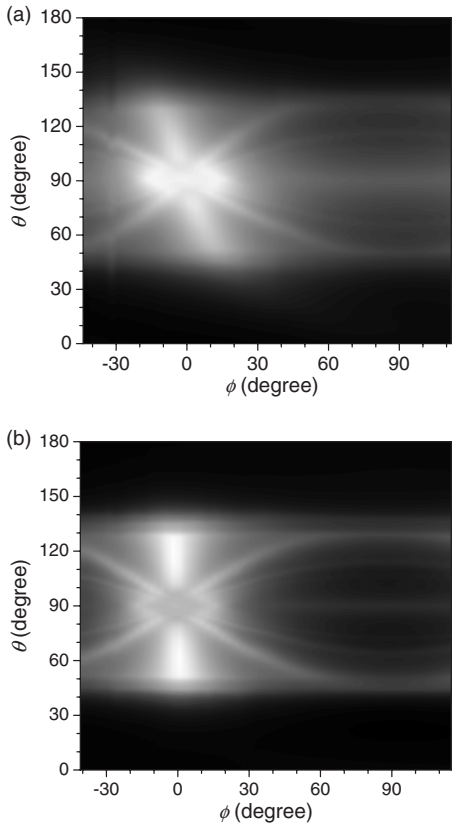

FIG. 5. (a) Equirectangular projections of $R_{xx}^{(\mathrm{II})}(\theta,\phi)$ and (b) $R_{zz}^{(\mathrm{II})}(\theta,\phi)$ of the recycled samples at a magnetic field of 10 T. Both of the sample pieces are from the sample used to measure $R_{xx}^{(\mathrm{I})}(\theta,\phi)$. The gray scale is between 5 and 47.5 Ω for $R_{xx}^{(\mathrm{II})}(\theta,\phi)$ and between 0.08 and 55 Ω for $R_{zz}^{(\mathrm{II})}(\theta,\phi)$, both on a logarithmic scale.

called the Bessel staircase, was found in studies of a superconducting qubit, which has a different physical nature, but is described by exactly the same equations as the interlayer transport in Q1D conductors.[34,35]

In summary, we have showed an unambiguous evidence that the three major MAEs of quasi-one-dimensional electron systems are only relevant to the interlayer part of resistance, at least for $(\mathrm{TMTSF})_2\mathrm{ClO}_4$. When the contribution from the interlayer magnetoresistance was properly removed, the intralayer resistance showed very weak and continuous azimuthal angle dependence and did not show any of the three major MAEs. We confirmed that such an observation was not an artifact related to the sample quality, because the same sample exhibited good quality resonances when the conventional way of making contacts was used or when the interlayer magnetoresistance was measured. In an independent experiment with $(\mathrm{TMTSF})_2\mathrm{PF}_6$, measurements of R_{yy} with contacts applied on sides of the sample, similar to the measurement for $R_{xx}^{(\mathrm{I})}(\theta,\phi)$, did not show any MAEs.

This work was supported by the Korea Science and Engineering Foundation (Grants Nos. F01-2006-000-10207-0 and R01-2007-000-20576-0). T. Osada is thanked for helpful discussions.

*Author to whom correspondence should be addressed; wkang@ewha.ac.kr

[1] T. Osada, A. Kawasumi, S. Kagoshima, N. Miura, and G. Saito, Phys. Rev. Lett. **66**, 1525 (1991).
[2] M. J. Naughton, O. H. Chung, M. Chaparala, X. Bu, and P. Coppens, Phys. Rev. Lett. **67**, 3712 (1991).
[3] W. Kang, S. T. Hannahs, and P. M. Chaikin, Phys. Rev. Lett. **69**, 2827 (1992).
[4] H. Kang, Y. J. Jo, S. Uji, and W. Kang, Phys. Rev. B **68**, 132508 (2003).
[5] G. M. Danner, W. Kang, and P. M. Chaikin, Phys. Rev. Lett. **72**, 3714 (1994).
[6] G. M. Danner and P. M. Chaikin, Phys. Rev. Lett. **75**, 4690 (1995).
[7] T. Osada, S. Kagoshima, and N. Miura, Phys. Rev. Lett. **77**, 5261 (1996).
[8] H. Yoshino and K. Murata, J. Phys. Soc. Jpn. **68**, 3027 (1999).
[9] I. J. Lee and M. J. Naughton, Phys. Rev. B **57**, 7423 (1998).
[10] I. J. Lee and M. J. Naughton, Phys. Rev. B **58**, R13343 (1998).
[11] W. Kang, T. Osada, Y. J. Jo, and H. Kang, Phys. Rev. Lett. **99**, 017002 (2007).
[12] A. G. Lebed, Pis'ma Zh. Eksp. Teor. Fiz. **43**, 137 (1986) [JETP Lett. **43**, 174 (1986)].
[13] S. P. Strong, D. G. Clarke, and P. W. Anderson, Phys. Rev. Lett. **73**, 1007 (1994).
[14] A. G. Lebed and N. N. Bagmet, Phys. Rev. B **55**, R8654 (1997).
[15] R. H. McKenzie and P. Moses, Phys. Rev. Lett. **81**, 4492 (1998).
[16] D. G. Clarke, S. P. Strong, P. M. Chaikin, and E. I. Chashechkina, Science **279**, 2071 (1998).
[17] T. Osada, Physica B **256-258**, 633 (1998).
[18] T. Osada, N. Kami, R. Kondo, and S. Kagoshima, Synth. Met. **103**, 2024 (1999).
[19] P. Moses and R. H. McKenzie, Phys. Rev. B **60**, 7998 (1999).
[20] T. Osada, Physica E (Amsterdam) **12**, 272 (2002).
[21] T. Osada, M. Kuraguchi, K. Kobayashi, and E. Ohmichi, Physica E (Amsterdam) **18**, 200 (2003).
[22] T. Osada, K. Kobayashi, and E. Ohmichi, Synth. Met. **135-136**, 653 (2003).
[23] A. G. Lebed and M. J. Naughton, Phys. Rev. Lett. **91**, 187003 (2003).
[24] U. Lundin and R. H. McKenzie, Phys. Rev. B **70**, 235122 (2004).
[25] A. G. Lebed, N. N. Bagmet, and M. J. Naughton, Phys. Rev. Lett. **93**, 157006 (2004).
[26] A. G. Lebed, H.-I. Ha, and M. J. Naughton, Phys. Rev. B **71**, 132504 (2005).
[27] B. K. Cooper and V. M. Yakovenko, Phys. Rev. Lett. **96**, 037001 (2006).
[28] S. J. Blundell and J. Singleton, Phys. Rev. B **53**, 5609 (1996).
[29] T. Osada, S. Kagoshima, and N. Miura, Phys. Rev. B **46**, 1812 (1992).
[30] K. Ishiguro, K. Yamaji, and G. Saito, *Organic Superconductors*, 2nd ed., Series in Solid State Science Vol. 88 (Springer-Verlag, Berlin, 1998).
[31] J. D. Wasscher, Philips Res. Rep. **16**, 301 (1961).
[32] H. C. Montgomery, J. Appl. Phys. **42**, 2971 (1971).
[33] C. Bergemann, J. Appl. Phys. **98**, 043707 (2005).
[34] W. D. Oliver, Y. Yu, J. C. Lee, K. K. Berggren, L. S. Levitov, and T. P. Orlando, Science **310**, 1653 (2005).
[35] D. M. Berns, W. D. Oliver, S. O. Valenzuela, A. V. Shytov, K. K. Berggren, L. S. Levitov, and T. P. Orlando, Phys. Rev. Lett. **97**, 150502 (2006).